Influence of solvation temperature on the molecular features and physical properties of fibroin membrane

Chuan Xin Liang and Kiyoshi Hirabayashi*

Department of Biopolymer Engineering, Faculty of Technology, Tokyo University of Agriculture and Technology, Koganei, Tokyo 184, Japan

(Received 6 June 1991; revised 25 October 1991; accepted 25 November 1991)

The effect of solvation temperature on the molecular features and physical properties of fibroin membranes were investigated. The physical properties discussed are elongation, strength, water absorbability, dynamic viscoelasticity and thermal stability. It was found that a molecular texture of fibroin which showed an i.r. spectral band at 655 cm^{-1} was not changed by a change in solvation conditions. However, the random coil, helical structure and β form conformation ratios, the molar mass and amino acid components of the fibroin samples prepared at various solvation temperatures were varied. As a result, the physical properties of the fibroin membrane were changed. Molecular conformations were studied by quantitative analysis of i.r. spectra and crystalline structures were confirmed by X-ray analysis. The variations in molar mass were elucidated by determining intrinsic viscosities of fibroin solutions. Changes in amino acid components were measured by amino acid analysis and ^{13}C n.m.r. spectroscopy. Further, fibroin membranes were characterized by determining their water contents, mechanical properties, and thermogravimetric and dynamic viscoelastic analyses.

(Keywords: fibroin membranes; quantitative analysis; molecular features; solvation temperature; physical properties)

INTRODUCTION

Recent studies[1–3] have shown that silk fibroin has good biological compatibility, which means that it has potential for application in artificial skin. Therefore, the study of fibroin membrane properties is important. Many other studies related to the structure of fibroin have indicated that the physical properties of the membrane are influenced by its structural features and casting conditions[4–7]. For instance, Pauling[6,7] suggested that the softness and water holding capacity of a given fibroin membrane might be controlled by its geometrical structure. However, the dependence of the fibroin membrane properties on molecular features has yet to be studied in detail. Recently, we found that the molecular character of solidified fibroin has a deep relationship with the physical properties of the membrane[8,9]. For example, high molecular orientation and a large molar mass in fibroin chains can bring about superior extension properties. Furthermore, the content of various characteristic amino acid residues, such as hydrophobic alanine and hydrophilic serine, have a strong influence on the water absorbability of fibroin membranes[10]. Therefore, in order to understand the conditions for preparing a membrane with the expected features, it is important to clarify the relationship between molecular features and properties of the membrane.

It was reported[11,12] that the molar masses of fibroin were different under various solvation conditions, although the reports did not go into detail on the dependence of molecular features. It was also suggested[11,12] that molecular conformations in regenerated fibroin solution were not changed during dialysis or by general casting methods[13]. Thus, it seems that the molecular features may be formed during the solvation process. Therefore, an understanding of the solvation mechanism and of the solvation temperature dependence of the molecular features is essential. However, few studies related to this problem have been reported.

Based on the above considerations, in this paper we quantitatively analyse the molecular characteristic variations of fibroin solubilized at different temperatures. The conformational transition mechanism and the relation between the physical properties of fibroin membrane and its molecular features are also studied.

EXPERIMENTAL

Samples

Cocoon was degummed using 0.5% $NaHCO_3$ solution and treated twice at 100°C for 30 min, before being washed with distilled water. Fibroin solution was prepared by dissolving (solvation conditions are given in *Table 1*) the degummed silk in 9.5 M lithium bromide. After dialysis with distilled water for 4 days, the solutions were centrifuged at 4000 rev min^{-1} for 20 min. Then the supernatant was collected and the concentration adjusted to 9.5 wt%. To keep the molecular conformations from being changed during the drying process[13], fibroin membranes were produced by casting the regenerated fibroin solutions on a polyethylene sheet at 5°C in air with 80% relative humidity. In order to obtain ^{13}C n.m.r.

*To whom correspondence should be addressed

0032-3861/92/204388-06

Table 1 Solvation temperature and solubilizing time of fibroin in 9.5 M LiBr aqueous solution

Sample	1	2	3	4	5	6
Solvation temperature (°C)	5	20	40	60	80	100
Solvation time (min)	3960	180	50	20	5	5

spectra, deuterium oxide was mixed with the fibroin solution in a ratio of 20 wt% (D_2O/solution). Samples for amino acid analysis were prepared by hydrolysing fibroin in 6 N aqueous HCl solution at 110°C for 48 h.

Measurements

When the membrane reached swelling equilibrium at 25°C and in air with 65% relative humidity, the strength and elongation were measured by a Toyo UTM-II tensile tester at a speed of 4 mm min^{-1}, and with a maximum load of ~50 N. The water contents were calculated by the following equation:

$$w = [(W_1 - W_0)/W_0] \times 100\% \quad (1)$$

where w is water content, and W_1 and W_0 are weights (mg) of membrane in the aforementioned soaked and dried (dried for 4 days at 120°C) states, respectively.

Dynamic mechanical spectra of membranes were carried out using a Toyo Baldwin DDV-II EA rheovibron at a frequency of 110 Hz and a heating rate of 2°C min^{-1}. Thermogravimetric analysis (t.g.a.) was carried out in air using a Shimadzu DT-30 thermal analyzer at a heating rate of 10°C min^{-1}. The decomposition temperatures and weight losses of membranes were evaluated by considering the intersecting point of the tangents of the t.g.a. curves.

The relative viscosity, E_{sp}, was determined using equation (2):

$$E_{sp} = (t/t_0) - 1 \quad (2)$$

The fall down time of fibroin solution (t) and distilled water (t_0) were measured with an Ostwald viscometer at 30°C. A straight line was obtained by plotting E_{sp}/c *versus* fibroin concentration c (g per 100 cm^3). The intrinsic viscosity was determined by considering the point of intersection of the E_{sp}/c axis and the straight line.

X-ray diffraction intensity curves of fibroin membranes were obtained using a Rigaku RAD-C wide-angle X-ray diffractometer operated at 40 kV and 30 mA using CuKα radiation. I.r. spectra were recorded on a Shimadzu IR-435 spectrophotometer at room temperature. The ratios of different molecular conformations were calculated[14] by reference to the areas of their characteristic peaks.

Amino acid analysis was carried out using a Shimadzu LC-5A liquid chromatograph at a flow rate of 500 μl min^{-1} at 55°C. ^{13}C n.m.r. spectra were run on a Nihon Denshi JNM-FX200 n.m.r. spectrometer operating at 50.1 MHz and 20°C using hexamethyldisiloxane (HMDS) as an internal reference. The spectral width was 12 004 Hz with 16.4 K data points. Since the delay time between pulses in the *FT*n.m.r. method must be five times the longest spin lattice relaxation time (T_1) for 99% relaxation[15], the pulse repetition rate was determined to be 2.12 s (because the longest T_1 was 0.41 s, measured at a concentration of 7.5 wt%)[16]. The relative ^{13}C n.m.r. spectral peak strength of carbons of amino acid residues was obtained using equation (3):

$$K = [(P_{s1}/P_{s0})] \times 100\% \quad (3)$$

where P_{s1} is the spectral peak strength of carbon atoms in amino acid residues and P_{s0} is that of HMDS.

RESULTS AND DISCUSSION

Solvation temperature dependence of molecular features of fibroin

The i.r. spectral region of 800–430 cm^{-1} was separated into seven bands. The bands for samples 1 and 6 are shown in *Figures 1a* and *b*, respectively. The molecular conformations are listed in *Table 2*. The absorption bands at 725 and 698 cm^{-1} are assigned to the β form[17], those at 540 cm^{-1} belong to the random coil[14] and the bands at 655 and 625 cm^{-1} are attributed to the α structure[12,14,17]. However, the molecular textural conformation is not yet clear. In our study, a fact which merits attention is that the 655 cm^{-1} band strengths were almost the same in all the samples. In other words, even

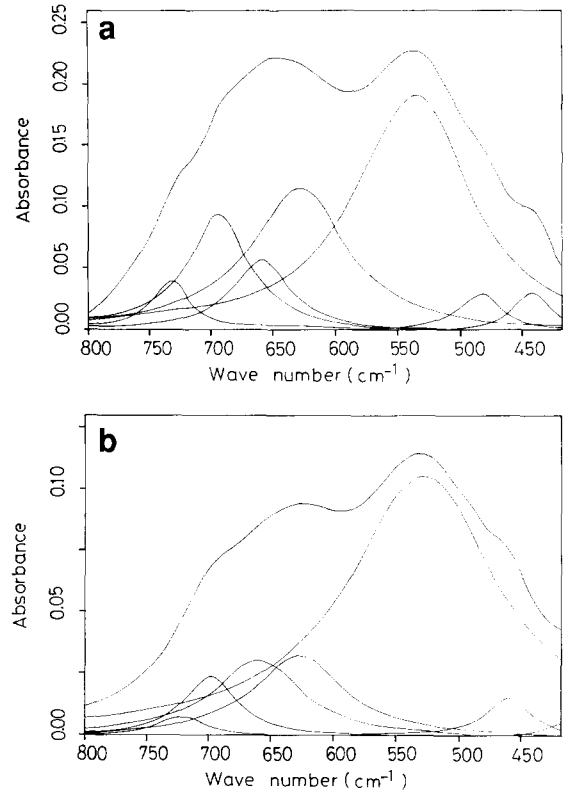

Figure 1 I.r. spectral domains of amides IV, V and VI of fibroin membranes and their separated peaks for samples 1(a) and 6(b)

Table 2 Molecular conformation contents (%) of fibroin membranes calculated from their i.r. spectral peak areas

Assignments	β form		α structure		Random coil
Wavenumber (cm^{-1})	725	698	655	625	540
Sample 1	3	18	10	34	45
2	3	16	11	22	48
3	2	13	14	19	52
4	2	10	13	19	56
5	2	5	13	17	63
6	1	4	12	14	69

if fibroin was solubilized under harsh conditions, this type of molecular structure was still not damaged. Thus, it is suggested that the molecular texture shown at 655 cm^{-1} is very stable. On the other hand, the absorbance at 625 cm^{-1} clearly decreased when the solvation temperature was above 80°C. Tsukada *et al.* reported that these bands might be attributed to the α helix[18]. However, we agree with the assignment suggested by Saito *et al.* that the 625 cm^{-1} bands should be assigned to a loose helical conformation[19,20]. The reason being that, if they are attributed to the α helix, then their content should not show a change[18]. Because the α helix is a very stable structure formed by intramolecular hydrogen bonds, it was difficult to damage compared with the helical structure.

An outstanding variation is that the random coil increased with a rise in solvation temperature whilst the β form gradually decreased. When the solvation temperature rose to 100°C, the random coil content increased to a maximum of ~70%, however, that of the β form decreased to ~5%. This indicated that the crystalline molecules were transformed from an oriented state to a random conformation accompanied by crystalline disintegration. X-ray diffractographs of fibroin membranes support this conjecture. *Figure 2* shows X-ray diffractographs and their separated crystalline peaks for samples 1 and 6. The peaks reflected from the (0 0 1) plane (9.7 Å) and from the (2 0 1) plane (4.3 Å) are assigned to the unique reflection of β crystal[18]. The diffractions at 7.6 and 5.5 Å belong to the α crystal. Since the decrease in α structure was less than that of the β crystal, the content of the former was increased relative to that of the latter. Nevertheless, as shown in *Figure 2* and *Table 3*, the β form peaks were weakened with a rise in solvation temperature. The reflection from the (0 0 1)

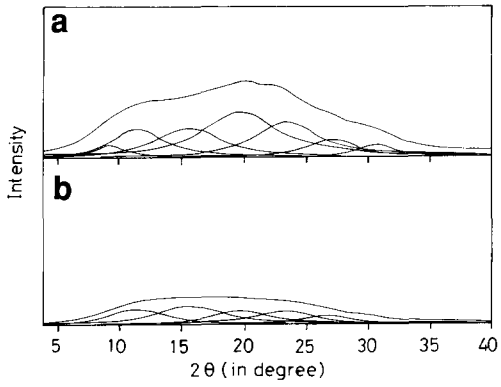

Figure 2 X-ray diffraction patterns of fibroin samples and their separated peaks for samples 1(a) and 6(b)

Table 3 Contents (%) of different crystal structures of fibroin membranes calculated from their X-ray diffraction peaks

Assignments	α structure				β form		
2θ	10.6	15.7	27.9	31.5	9.2	20.6	24.8
Sample 1	15	19	7	4	3	32	20
2	15	19	7	4	3	32	20
3	17	22	7	4	2	28	20
4	18	27	8	4	2	21	20
5	20	30	9	3	1	18	19
6	22	31	10	3	0	16	18

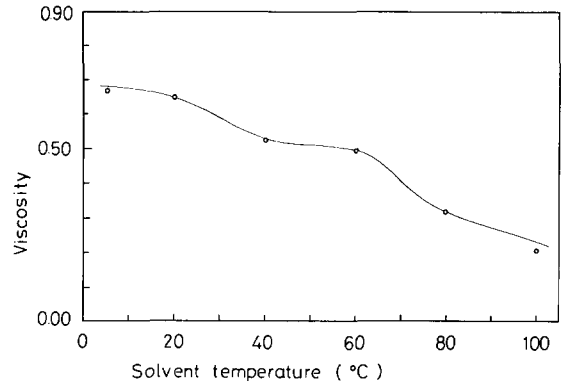

Figure 3 Solvation temperature dependence of intrinsic viscosities of regenerated fibroin solutions

plane even disappeared in sample 6. These results indicate that both the amorphous and crystal regions were damaged at high solvation temperatures. The reason for this is that the lithium ions can easily enter the crystal domain by active ionic movements, so that the peptide chains are broken by co-ordination between lithium ions and polar tyrosine and serine[21]. Simultaneously, when more and more water molecules were adsorbed on the polar groups (such as CO and NH) of peptides, the intermolecular hydrogen bonds were weakened or broken[22]. However, the crystal region was not totally damaged at low solvation temperature. This is because the movement of water molecules and lithium ions is so weak that only some of them enter the crystal domain. As a result, only a few peptide chains and intermolecular bands were broken. Therefore, the highest and lowest intrinsic viscosities (*Figure 3*) were found when the solvation temperature was 5°C or above 80°C, respectively, as expected from the above discussion. This indicated that the molar mass was lowered with a rise in solvation temperature.

With respect to the crystalline disintegration it should be remembered that a deposition phenomenon was shown in the dialysis process. We found that this behaviour occurred only in the solution prepared at high solvation temperature. The reason for this is not yet very clear, but a possible source is that hydrophobic residues of disintegrated crystal fragments mutually formed hydrophobic bonds when they were excluded from water molecules due to the strong cohesion of water[23]. It is known that alanine, glycine and serine mainly exist in the crystal domain[24]. Thus, it seems that the deposition was induced by hydrophobic bonding between the crystalline residues. In fact, the amino acid analysis (*Table 4*) showed that the component ratios of hydrophobic alanine, glycine and hydrophilic serine were reduced when the solvation temperature was above 80°C. Since the ^{13}C n.m.r. spectral peak strength is proportional to the number of carbon atoms[25], as seen from *Table 5*, the relative ^{13}C n.m.r. spectral peak strengths also gave the same results. The decrease in hydrophilic serine suggests that the serines are arranged inside the microcrystal unit[24].

Solvation temperature dependence of physical properties of fibroin

Thermal stabilities. Figure 4 shows the t.g.a. thermograms of fibroin membranes. All samples showed two

Table 4 Amino acid composition (mol%) of regenerated fibroin solution solubilized in 9.5 M LiBr aqueous solution

Sample	1	2	3	4	5	6
ASP	1.40	0.92	0.98	0.96	1.59	1.50
THR	0.71	0.51	0.68	0.66	0.95	0.96
SER	10.01	10.32	10.09	10.11	9.31	9.32
GLU	1.27	1.07	1.22	1.21	1.55	1.55
PRO	0.30	0.40	0.30	0.34	0.49	0.48
GLY	44.77	44.76	44.51	44.53	42.88	42.34
ALA	31.75	31.58	31.64	3.167	30.55	29.96
CYS	0.17	0.23	0.16	0.20	0.26	0.22
VAL	1.19	1.03	1.03	1.23	1.57	1.87
MET	0.10	0.14	0.15	0.12	0.19	0.15
ILE	0.50	0.71	0.81	0.80	0.97	0.91
LEU	0.38	0.63	0.67	0.57	0.73	0.70
TYR	5.85	5.95	5.88	5.85	6.36	7.47
PHE	0.93	1.07	1.05	1.06	1.60	1.53
LYS	0.16	0.24	0.29	0.22	0.30	0.28
HIS	0.13	0.19	0.16	0.17	0.17	0.18
ARG	0.38	0.25	0.38	0.30	0.53	0.58

Table 5 Relative ^{13}C n.m.r. spectral peak strengths (%) for the carbon atoms of four amino acid residues of fibroin

Sample		1	2	3	4	5	6
Gly	C_α	68.51	68.42	68.52	68.47	64.27	64.25
Ala	C_α	72.49	72.46	72.51	72.55	64.46	64.45
	C_β	85.10	85.12	85.06	85.09	83.89	83.86
Ser	C_α	30.48	30.43	30.42	30.41	28.03	28.00
	C_β	30.29	30.27	30.18	30.22	29.08	28.38
Tyr	C_δ	28.75	28.72	28.87	28.85	30.89	31.08
	C_ε	27.41	27.45	27.47	27.94	31.06	31.10
	C_β	13.38	13.29	13.27	13.93	16.26	16.45

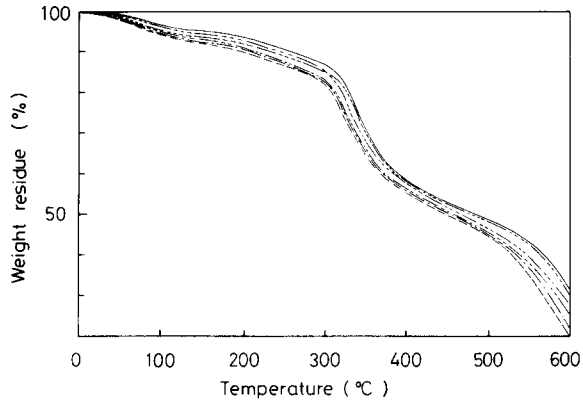

Figure 4 T.g.a. therograms of fibroin membranes: (——) sample 1; (— - - -) sample 2; (— — —) sample 3; (— — —) sample 4; (— —) sample 5; (— — —) sample 6

stages of active weight loss at elevated temperature. The majority of weight loss was found to occur in the temperature range of 250–400°C (stage 1) which is attributed to the disintegration of intermolecular side chains in the crystalline melting process[26]. Stage 2 at 440–600°C is defined as a secondary decomposition attributed to the main chain disintegration with simultaneous carbon atom rearrangements[26]. The residual weight and high primary and secondary decomposition temperature were decreased when the solvation temperature was increased. In particular, the secondary decomposition temperature of sample 6 was lower than that of samle 1 by 31°C. The t.g.a. data (*Table 6*) indicated that the thermal stabilities of fibroin membranes were controlled by the β form contents and their crystallinities.

Dynamic viscoelasticities. The dynamic storage modulus decreased with increase in solvation temperature (*Figure 5*). In contrast, the loss modulus increased. A remarkable increase in loss modulus was found when the solvation temperature was 100°C. These variations in dynamic viscoelasticities were in response to the molecular weight and molecular conformation changes of fibroin. It is clear from *Figure 5*, that when the solvation temperature is increased, the dispersion a and peaks b were shifted gradually to lower temperatures. Moreover, the maximum increment of peak a′ of the loss modulus was found for

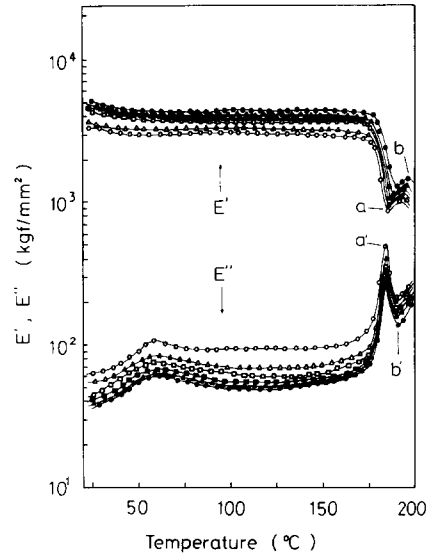

Figure 5 Solvation temperature dependence of dynamic modulus and loss modulus of fibroin membranes: (●) sample 1; (▲) sample 2; (■) sample 3; (□) sample 4; (△) sample 5; (○) sample 6

Table 6 Thermal properties of fibroin membranes

Sample	1	2	3	4	5	6
Primary decomposition						
Temperature (°C)	315	314	312	308	304	302
Weight loss (%)	12.1	13.5	14.2	15.0	15.3	15.5
Secondary decomposition						
Temperature (°C)	557	554	544	539	534	526
Weight loss (%)	55.6	56.8	58.0	59.1	59.6	59.8

sample 6. The dispersions at a were contributions from movements of crystal chains[27]. In other words, the dispersions were induced by broken intra- or intermolecular hydrogen bonds. The peaks b and b' were caused by the crystallization behaviour[27–29]. The changes in the characteristic dispersions and peaks of the dynamic mechanical spectra were caused by the crystallinity and molecular orientation of fibroin.

Water holding capacity. It was reported that the water holding capacity of fibroin membrane might be influenced by the effect of crystallinity, the hydrophilic residue content and intermolecular hydroben bonds[30,31]. The lowest water content was found when the solvation temperature was 5°C or 100°C (*Table 7*). The reason for the former is that the polar groups of peptides cannot easily absorb much water, because the β and α structures are much more than random coil conformations of fibroin. That is, the polar groups participating in intra- or intermolecular hydrogen bonds are more than free polar groups. A second possible cause may be due to the earlier discussion, that is, since the hydrophilic serines are arranged inside the microcrystal units they cannot come into contact with water molecules. In the latter case, the reduction of water content was attributed to the decrease in hydrophilic serine (*Table 5*). On the other hand, the highest water content was found when the solvation temperature was 60°C. This is due to the increase in the amorphous region and the random coil conformation. Thus, it seems that the hydrophilicity of fibroin membrane mainly depends on the number of hydrophilic amino acid residues and the amount of amorphous domain.

Table 7 Water contents of fibroin membranes

Sample	1	2	3	4	5	6
Water content (%)	13.9	14.2	14.9	15.9	15.6	13.9

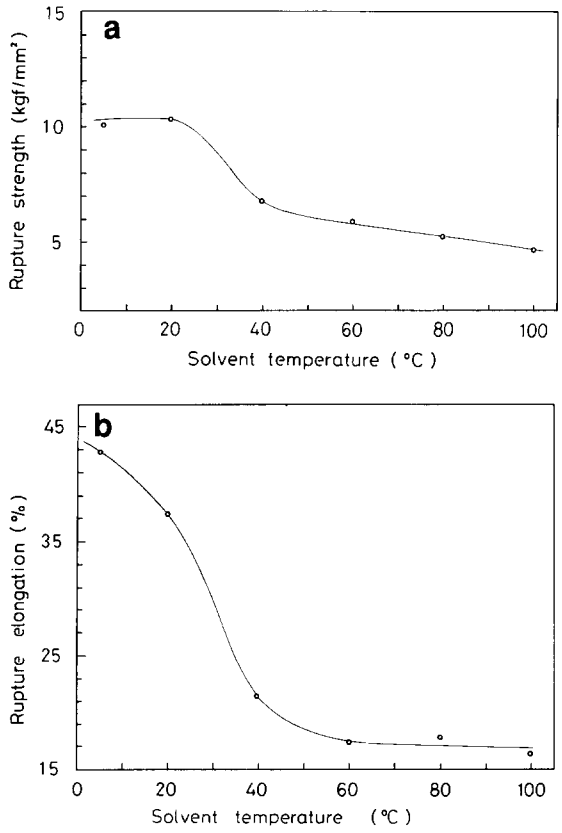

Figure 6 Relationship between (a) the rupture strength and (b) the elongation at break of fibroin membranes and the solvation temperature

Mechanical properties. When the solvation temperature was below 20°C, the fibroin membranes showed the highest rupture strength (~ 50 N mm^{-2}) which suddenly decreased with increase in solvation temperature, and gradually tended towards a constant (*Figure 6a*). One reason for the high rupture strength is that, as also clear from the intrinsic viscosities (*Figure 3*), there are only a few broken peptide chains. Another cause is, as found from the high β form ratio, that many intermolecular hydroben bonds remained. In contrast, the low rupture strength was due to the low molar mass and the high random coil conformation content. In concert with the rupture strength, the rupture elongation of fibroin membranes also decreased with increase in solvation temperature (*Figure 6b*). Sample 1 shows the highest rupture elongation. This is due to good ductility induced by the high molar mass and high molecular orientation. However, the rupture elongation was remarkably decreased when the solvation temperature was above 20°C. A cause for this is that the ductility of the membrane decreased in accordance with the lowering of the molar mass.

CONCLUSIONS

The random coil molecular conformation of fibroin increased when the solvation temperature was increased. The highest random coil content (69%) was found in sample 6. However, the highest molar mass and β form content (18%) in fibroin were shown for samples made at low solvation temperature. Moreover, the hydrophobic amino acid residues, such as alanine, glycine, and hydrophilic serine were decreased when the solvation temperature was above 60°C. Accordingly, the high rupture strength, excellent rupture elongation, thermal stabilities and good dynamic storage modulus were obtained by solubilizing fibroin at low temperature. The high hydrophilicity of fibroin membranes can be induced by a large amorphous domain and the presence of more hydrophilic amino acid residues.

REFERENCES

1 Kuzuhara, A., Asakura, T., Tomoda, R. and Matsunaga, T. *J. Biotechnol.* 1987, **5**, 199
2 Grasset, L., Cordier, D., Couturier, R. and Ville, A. *Biotechnol. Bioeng.* 1983, **25**, 1423
3 Grasset, L., Cordier, D. and Ville, A. *Biotechnol. Bioeng.* 1977, **19**, 611
4 Magoshi, J., Kasai, Y. and Kakudo, M. *Chem. Soc.* 1973, **30**, 649
5 Hagiwara, M. and Ishikawa, K. *Sen-i Gakkasiahi* 1976, **32**, 206
6 Pauling, L. *Sen-i Gakkaishi* 1945, **67**, 555
7 Pauling, L. and Corey, R. B. *Chem. Soc.* 1950, **72**, 5349
8 Liang, C. X. and Hirabayashi, K. *Sen-i Gakkaishi* 1990, **46**, 181
9 Liang, C. X. and Hirabayashi, K. *J. Appl. Pllym. Sci.* in press
10 Yanou, Y. in 'Structure of Silk Fiber' (Ed. T. Itou), Chikuma Kai, Nagano, Ueda, 1957, p. 226 (in Japanese)
11 Hayashi, K. in 'Structure of Silk Fiber' (Ed. T. Itou), Chikuma Kai, Nagano, Ueda, 1957, p. 340 (in Japanese)

12 Mizushima, S. and Shimanouchi, Y. in 'Structure of Silk Fiber' (Ed. T. Itou), Chikuma Kai, Nagano, Ueda, 1957, p. 448 (in Japanese)
13 Magoshi, J., Mizuide, M., Magoshi, Y., Takahashi, K., Kudo, M. and Nakamura, S. *J. Polym. Sci., Polym. Phys. Edn* 1979, **17**, 515
14 Liang, C. X. and Hirabayashi, K. *J. Polym. Sci., Polym. Phys. Edn* submitted
15 De Pooter, M., Smith, P. B., Dohrer, K. K., Bennett, K. F., Meadows, M. D., Smith, C. G., Schouwenaar, H. P. and Geerards, R. A. *J. Appl. Polym. Soc.* 1991, **42**, 399
16 Asakura, T., Watanabe, Y., Uchida, A. and Minagawa, H. *Macromolecules* 1984, **17**, 1075
17 Konishi, T. and Kurokawa, M. *Sen-i Gakkaishi* 1968, **24**, 550
18 Tsukada, M., Nagura, M. and Ishikawa, H. *Sen-i Gakkasihi* 1984, **24**, 231
19 Marsh, R. E., Corey, R. B. and Pauling, L. *Biochem. Biophys. Acta* 1955, **16**, 1
20 Saito, H., Tabeta, R., Asakura, T., Iwanaga, Y., Shoji, A., Ozaki, T. and Ando, I. *Macromolecules* 1984, **17**, 1405
21 Ajisawa, A. *J. Seric. Sci. Jpn* 1969, **38**, 365
22 Mizushima, S. and Shimanouchi, Y. in 'Structure of Silk Fiber' (Ed. T. Itou), Chikuma Kai, Nagano, Ueda, 1957, p. 263 (in Japanese)
23 Tamamushi, B., Fujiyama, O., Kotani, M., Ando, E., Takahashi, H., Kubo, R., Nagakura, S. and Inoue, T. 'Rikagaku jiten', Iwanami shoten, Tokyo, 1981, p. 760 (in Japanese)
24 Lucas, F., Shaw, J. T. B. and Smith, S. G. *Adv. Protein Chem.* 1958, **13**, 107
25 Kemp, W. 'NMR in Chemistry – A Multinuclear Introduction', Macmillan, London, 1986, p. 98
26 Hirabayashi, K., Suzuki, T., Nagura, M. and Ishikawa, H. *Bunseki kiki* 1974, **12**, 437
27 Magoshi, J. *J. Mater. Sci.* 1973, **22**, 499
28 Magoshi, J. *J. Polym. Soc.* 1974, **31**, 456
29 Ishikawa, H., Sofue, E. and Matuzaki, T. 'The Study Report of Textile Science and Technology', Vol. 10, Shinshu University, 1960, p. 176
30 Goodings, A. C. and Turl, L. H. *J. Text. Inst.* 1940, **31**, 69
31 Matano, N. and Ozawa, Y. *Chem. Inst.* 1940, **40**, 996